Joint SRME and model-based water-layer demultiple for ocean bottom node

Hui Huang, Ping Wang, Jing Yang, Hui Chen (CGG);*
Pierre-Olivier Ariston, Imtiaz Ahmed, and Nick Bassett (BP)

Summary

Ocean bottom node (OBN) SRME that combines OBN and streamer data is known to be an effective way to predict surface-related multiples in OBN data. However, the available streamer data often have limited offset/azimuth coverage. Additionally, the double source wavelets due to the convolution of OBN and streamer data limit the bandwidth (loss of low and high frequency) of the predicted multiples. OBN model-based water-layer demultiple (MWD) overcomes such limitations and is a good complement of OBN SRME; MWD replaces the streamer data with the water-bottom Green's function that has no offset/azimuth limitation and keeps the full bandwidth of the input data. With Gulf of Mexico (GOM) OBN data over the Atlantis field, we illustrate the benefit of joint SRME and MWD over SRME alone with the improved attenuation of low-frequency multiples and water layer-related multiples.

Introduction

Ocean bottom node (OBN) acquisition is increasingly being used for seismic imaging and monitoring of reservoirs. Its ultra-long offset and full azimuth coverage and good low-frequency signals provide the potential to better illuminate the subsurface, especially in geologically complicated regions. However, as with streamer data, multiple attenuation is a critical component of an OBN data processing flow. A multiple attenuation strategy that can handle ultra-long offset/full-azimuth data and low-frequency multiples is important to take full advantage of the inherent benefits of OBN data.

Surface-related multiple elimination (SRME) has been used on surface-streamer data with varying degrees of success. However, it requires significant modifications to work with OBN data due to the sparse sampling of the receivers (nodes) and the significant datum difference between sources and receivers. To address such issues, a modified SRME scheme was proposed by Ikelle (1999) and Verschuur and Neumann (1999), in which OBN and streamer data were combined to predict surface-related multiples for OBN data (Zhong et al., 2014). Like surface-streamer SRME, the OBN SRME also suffers from limited offset and azimuth coverage of streamer data and limited bandwidth due to an extra source wavelet.

Wang et al. (2011) proposed model-based water-layer demultiple (MWD) for surface-streamer data, and it was subsequently extended to OBN acquisition (Jin and Wang, 2012). Instead of convolving OBN data with streamer data as in OBN SRME, OBN MWD convolves the OBN data with the water-bottom Green's function modeled from a given water-layer model, and therefore does not suffer from a lack of streamer data at near/far offsets and avoids the extra source wavelet issue. As a result, the MWD model has a more correct frequency spectrum and relative amplitude than the SRME model, which makes the subtraction easier. A similar method has been proposed to predict the source-side water layer-related multiples through wavefield extrapolation (Xia et al., 2006). However, all these methods only predict a subset of the surface-related multiples and thus need to be combined with SRME to handle all the surface-related multiples (Wang et al., 2011).

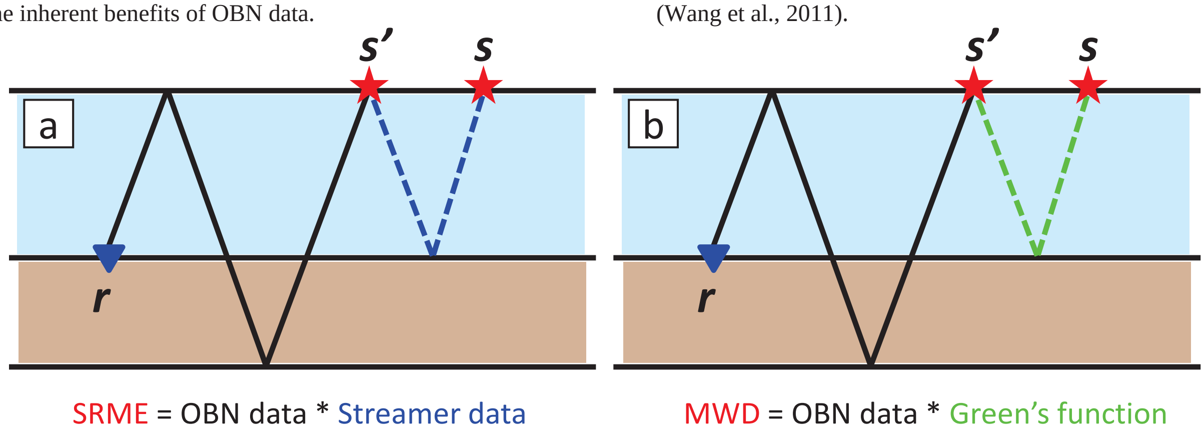

Figure 1: Schematics of (a) SRME and (b) MWD model prediction for OBN data. The SRME model between a source ***s*** and a receiver ***r*** is calculated from the convolution of the OBN data between ***s'*** and ***r*** and the streamer data between ***s*** and ***s'***. The MWD model is calculated from the convolution of OBN data between ***s'*** and ***r*** and the water-bottom Green's function between ***s*** and ***s'***.

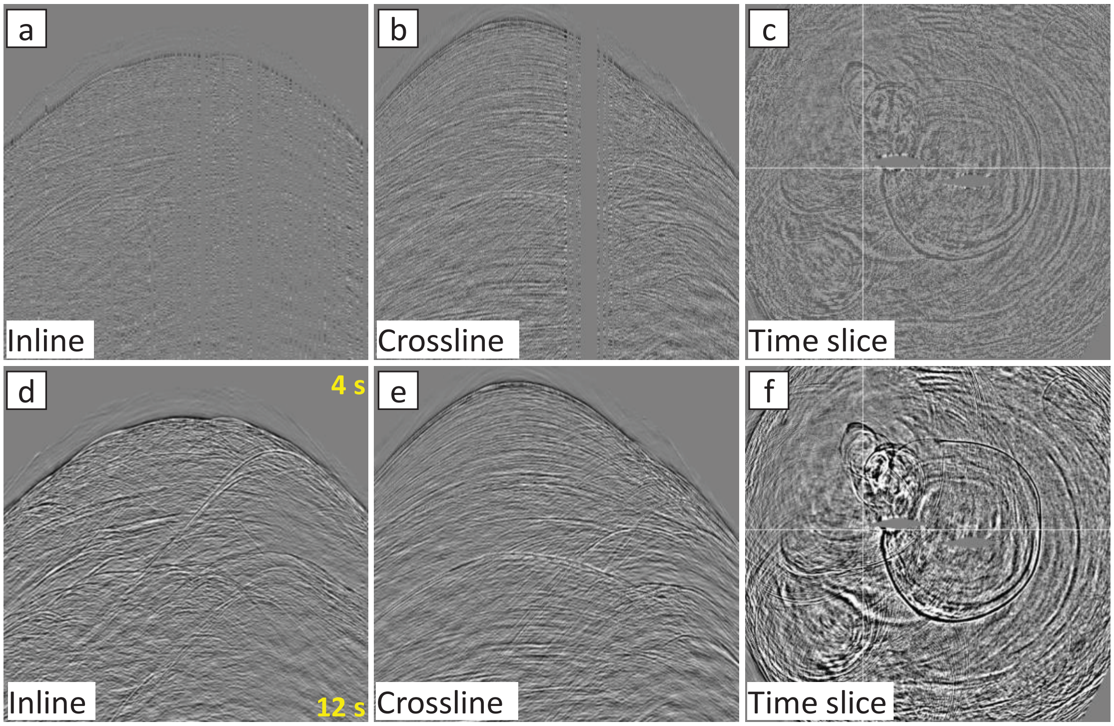

Figure 2: OBN gather before (50m×50m) and after (12.5m×12.5m) interpolation: (a), (b), (c): the inline, crossline, and time-slice views of an OBN gather before interpolation; (d), (e), (f): the same node gather after interpolation. The thin vertical and horizontal white lines in the time slices show the location of inline and crossline, respectively. The time slice is at 7.5 s. Note that the three figures before interpolation (a), (b), and (c) are gained up 6 dB for easier comparison with those after interpolation (d), (e), and (f).

In this paper, we propose a demultiple workflow for OBN data. First, both the OBN and streamer data are regularized and interpolated to a denser sampling grid in order to reduce artifacts by aliased signals. Then, an SRME model is predicted by convolving the regularized OBN data with the streamer data, and an MWD model is predicted by convolving the regularized OBN data with a calculated Green's function from a given water-layer model. Finally, both the SRME and MWD models are jointly subtracted from the input data to take advantage of both multiple models. We demonstrate the effectiveness of this approach using deep-water GOM OBN data over the Atlantis field.

Method

One strategy to mitigate the loss of bandwidth due to double source wavelets is to extend the bandwidth of the OBN and streamer data. This can be achieved by applying shot and shot/receiver deghosting to the OBN and streamer data, respectively (Posthumus, 1993; Wang et al., 2014).

To reduce artifacts from aliased signals, both the OBN before multiple attenuation and streamer data after surface multiple attenuation (to mitigate the cross-talk among multiples in both OBN and streamer data) are interpolated to a denser sampling grid. This is accomplished with streamer data using the anti-leakage Fourier transform method (Xu et al., 2005), and with OBN data using the progressive sparse Tau-P inversion method (Wang and Nimsaila, 2014); the sparse Tau-P inversion adequately handles the strong spatial aliasing characteristic of OBN acquisition (e.g., 50m×50m shot spacing). Figure 2 shows an OBN gather before and after interpolation. Small holes are filled by interpolation. The events look more continuous and coherent after interpolation.

After deghosting, regularization and interpolation, the next step is to predict the multiple models, which we do for SRME and MWD individually. With the regularized/interpolated streamer data, $\boldsymbol{P}$, and OBN data, $\boldsymbol{O}$, we obtain the SRME model (Figure 1a) as follows (Ikelle, 1999; Verschuur and Neumann, 1999):

$$M_{SRME}(\omega;\boldsymbol{r},\boldsymbol{s}) = -i\omega \int O(\omega;\boldsymbol{r},\boldsymbol{s}')P(\omega;\boldsymbol{s}',\boldsymbol{s})d\boldsymbol{s}', \quad (1)$$

where $\boldsymbol{\omega}$ is the angular frequency, $\boldsymbol{r}/\boldsymbol{s}$ is receiver/source location, and $\boldsymbol{s}'$ is the surface integration grid.

Similarly, the MWD model (Figure 1b) can be written as (Jin and Wang, 2012):

$$M_{MWD}(\omega;\boldsymbol{r},\boldsymbol{s}) = -i\omega\int O(\omega;\boldsymbol{r},\boldsymbol{s}')G(\omega;\boldsymbol{s}',\boldsymbol{s})d\boldsymbol{s}', \quad (2)$$

where G is the Green's function computed using a given water-layer model through wave-equation modeling.

Theoretically, the SRME model given by Equation 1 includes all the surface-related multiples. It also would not exhibit much cross-talk noise due to the prior removal of multiples in the streamer data. However, its effectiveness at modeling multiples in the OBN data is still limited by the following two factors:

1. Streamer data have limited offsets (no near or ultra-long offsets) and azimuth coverage;
2. Double source wavelets limit the bandwidth.

On the other hand, the MWD model given by Equation 2 overcomes the above limitations by replacing the streamer data with the water-bottom Green's function, which models data at any offset and azimuth with a white spectrum. However, it predicts only the water layer-related multiples. To model all surface-related multiples in practice, both the SRME and MWD models are predicted and jointly subtracted from the input data (Wang et al., 2011).

Application to Atlantis OBN data

Figure 3 shows the differences of SRME and MWD models, modeled with the same integration aperture ($\boldsymbol{s}'$ in Equations 1 and 2). The yellow arrows in Figures 3a-3b highlight two events predicted by SRME but not by MWD - likely not water layer-related multiples. A water layer-related multiple event with strong energy is highlighted by red arrows in the lower section. Despite the large aperture used, this multiple is not well predicted by SRME (Figure 3b), while MWD nicely predicted this multiple using the same aperture (Figure 3c). It is possible that the data needed to predict this multiple were not fully recorded in the streamer data.

The SRME model also has narrower bandwidth than the input data (inset of Figure 3c). The convolution of the OBN and streamer data results in two source wavelets in the multiple model, one from the OBN data and one from the streamer data. Consequently, the SRME model loses energy at both the low- and high-frequency ends. However, the MWD model is the convolution of the OBN data with a white Green's function; therefore, it matches the frequency spectrum of the input data. Figures 3d-3f show the input and two multiple models high-cut at 8 Hz. In general, the MWD model is more coherent and better matches the input data. Multiples highlighted by blue arrows are better predicted in the MWD model (Figure 3f) than in the SRME model (Figure 3e).

The final step in our workflow is to jointly subtract both the SRME and MWD models from the input data (Figures 4c and 4f). Figure 4b shows the demultiple result using only

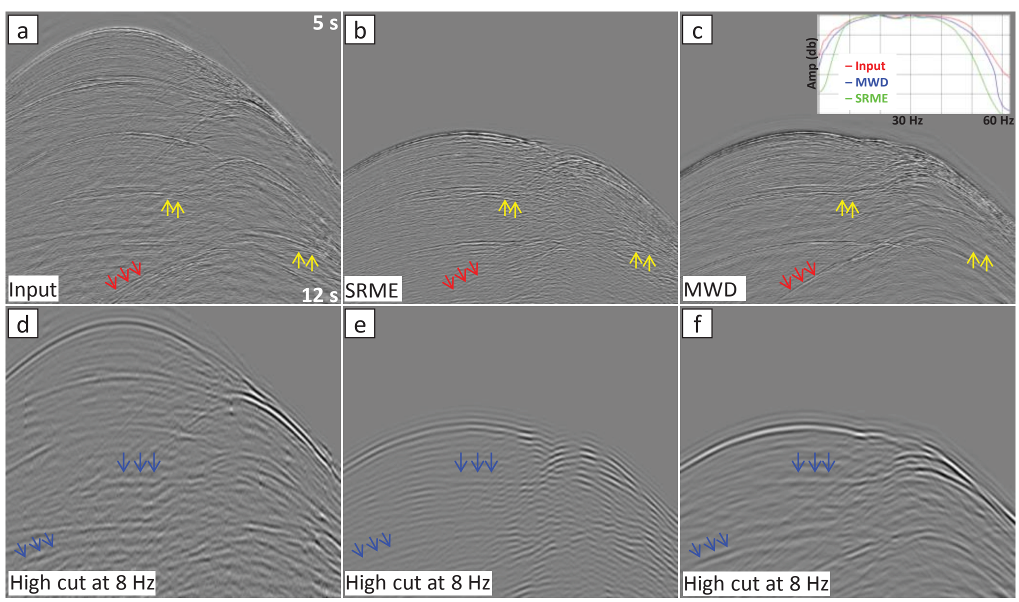

Figure 3: OBN input and two multiple models for a shot line: (a) input; (b) SRME model; (c) MWD model; (d), (e), (f): (a), (b), (c) high-cut at 8 Hz. The red arrows highlight a water layer-related multiple event which is better predicted in MWD model. The blue arrows show two low-frequency multiple events that are better predicted in the MWD model. The yellow arrows highlight two events only predicted in the SRME model. The inset is the frequency spectra of the input and two multiple models. The SRME model loses energy at both low- and high-frequency ends due to the dual source wavelets.

the SRME model. The water layer-related multiple highlighted by red arrows is not well attenuated due to poor prediction (Figure 3b). On the contrary, the same multiple is nicely attenuated by joint SRME and MWD subtraction (Figure 4c) because it was well predicted by MWD (Figure 3c). Figures 4e and 4f show results high-cut at 8 Hz. We observed that joint SRME and MWD attenuates better low-frequency multiples than SRME only (blue arrows). For the events only predicted in the SRME model, the joint demultiple flow shows the same results as that using SRME model only (yellow arrows in Figure 4b and c).

Discussions and Conclusions

The effectiveness of OBN SRME is limited by the incomplete offset/azimuth coverage of streamer data and double source wavelets due to convolution of OBN and streamer data. OBN MWD overcomes such limitations by replacing streamer data with the modeled water-bottom Green's function that provides data at any offset/azimuth with a white spectrum. However, OBN MWD only predicts the water layer-related multiples, and therefore needs to be combined with SRME. With Atlantis OBN data, we demonstrate that OBN MWD can predict water layer-related multiples for deep events that are not predicted by OBN SRME. Because MWD honors the spectrum of the input data, it can predict low-frequency water layer-related multiples better than SRME. This is significant in that it enables us to better use the good low-frequency signals present in OBN data.

The OBN and streamer data used here were after shot and shot/receiver deghosting, respectively. Deghosting could extend the bandwidth of both the OBN and streamer data and therefore mitigate the negative impact of double source wavelets in OBN SRME. Nevertheless, we found MWD still performed better than SRME for water layer-related multiples at the low-frequency end because it more closely matched the input spectrum.

Li et al. (2015) observed that OBN data could have large wavelet variations across azimuths and offsets due to source array directivity. Ideally, such wavelet variations need to be normalized before SRME and MWD. One possible solution for this could be a directional designature method for OBN data (Wang et al., 2015). This method requires gun-array nearfield hydrophone measurements that are readily available for most of the recent acquisitions.

Acknowledgements

We thank BP, BHP and the Shenzi and Neptune partnerships, and CGG for permission to publish this work. We also thank Melanie Vu and Jenny Qin for testing the algorithm and Rongxin Huang for constructive discussions.

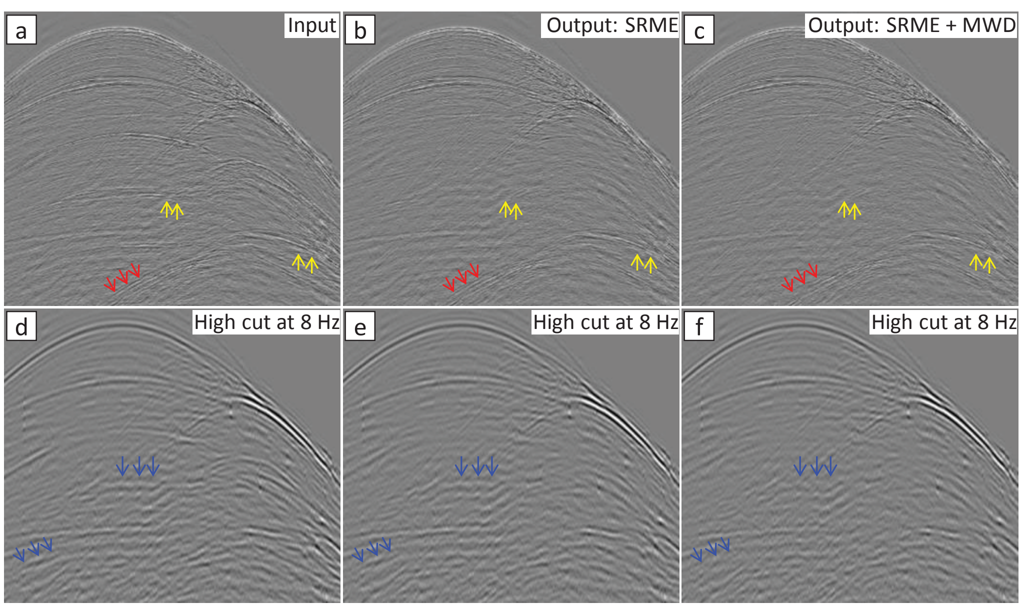

Figure 4: Demultiple input and output: (a)input; (b) output using the SRME model only; (c) output jointly using the SRME and MWD models; (d), (e), (f) : (a), (b), (c) high-cut at 8 Hz. The joint demultiple flow better attenuates water layer-related multiples (red arrows) and multiples at low frequencies (blue arrows). The yellow arrows show that the two multiples predicted only in the SRME model (same as in Figure 3) are well attenuated, and the joint demultiple flow shows the same attenuation output as that using the SRME model only.

EDITED REFERENCES

Note: This reference list is a copyedited version of the reference list submitted by the author. Reference lists for the 2016 SEG Technical Program Expanded Abstracts have been copyedited so that references provided with the online metadata for each paper will achieve a high degree of linking to cited sources that appear on the Web.

REFERENCES

Ikelle, L. T., 1999, Combining two seismic experiments to attenuate free-surface multiples in OBC data: Geophysical Prospecting, **47**, 179–193, http://dx.doi.org/10.1046/j.1365-2478.1999.00125.x.

Jin, H., and P. Wang, 2012, Model-based water-layer demultiple (MWD) for shallow water: from streamer to OBS: 82nd Annual International Meeting, SEG, Expanded Abstracts, 1–5, http://dx.doi.org/10.1190/segam2012-1401.1.

Li, X., J. Yang, H. Chen, M. Vu, and P. Wang, 2015, Application of 3D source deghosting and designature to deep-water ocean bottom node data: 85th Annual International Meeting, SEG, Expanded Abstracts, 5634–5638, http://dx.doi.org/10.1190/segam2015-5924634.1.

Posthumus, B. J., 1993, Deghosting using a twin streamer configuration: Geophysical Prospecting, **41**, 267–286, http://dx.doi.org/10.1111/gpr.1993.41.issue-3.

Verschuur, D., and E. Neumann, 1999, Integration of OBS data and surface data for OBS multiple removal: 69th Annual International Meeting, SEG, Expanded Abstracts, 1350–1353.

Wang, P., H. Jin, S. Xu, and Y. Zhang, 2011, Model-based water-layer demultiple: 81st Annual International Meeting, SEG, Expanded Abstracts, 3551–3555, http://dx.doi.org/10.1190/1.3627937.

Wang, P., and K. Nimsaila, 2014, Fast progressive sparse tau-p transform for regularization of spatially aliased seismic data: 84th Annual International Meeting, SEG, Expanded Abstracts, 3589–3593, http://dx.doi.org/10.1190/segam2014-0889.1.

Wang, P., K. Nimsaila, Z. Dongping, Z. Fu, H. Shen, G. Poole, and N. Chazalnoel, 2015, Joint 3D source-side deghosting and designature for modern air-gun arrays: 77th Annual International Conference and Exhibition, EAGE, Extended Abstracts, http://dx.doi.org/10.3997/2214-4609.201413190.

Wang, P., S. Ray, and K. Nimsaila, 2014, 3D joint deghosting and crossline interpolation for marine single-component streamer data: 84th Annual International Meeting, SEG, Expanded Abstracts, 3594–3598, http://dx.doi.org/10.1190/segam2014-0882.1.

Xia, G., R. Clark., J. Etgen, N. Kabir, K. Matson, and S. Michell, 2006, OBS multiple attenuation with application to the deepwater GOM Atlantis OBS node data: 76th Annual International Meeting, SEG, Expanded Abstracts, 2654–2658, http://dx.doi.org/10.1190/1.2370073.

Xu, S., Y. Zhang, D. Pham, and G. Lambare, 2005, Anti-leakage Fourier transform for seismic data regularization: Geophysics, **70**, no. 4, V87–V95, http://dx.doi.org/10.1190/1.1993713.

Zhong, R., J. Chao, S. Ji, and Y. Xuan, 2014, Incorporating streamer data for OBN free-surface multiple prediction — A case study in deep-water Gulf of Mexico: 84th Annual International Meeting, SEG, Expanded Abstracts, 4108–4112, http://dx.doi.org/10.1190/segam2014-0322.1.